

Fast Synthesis of Nano $[\text{Co}_3(\text{BTC})_2]$ and $[\text{Zn}_3(\text{BTC})_2]$ MOFs by Mechano Ball-Milling method and Characterization: Dyes Adsorption Efficacy and Antimicrobial Studies

Chinthamreddy Amaravathi^{1,2}, Katari Naresh Kumar¹ and Manubolu Surya Surendra Babu^{1*}

1. Department of Chemistry, School of Science, GITAM University, Hyderabad Campus, Hyderabad 502 329, INDIA

2. Department of Chemistry, CMR Technical Campus, Hyderabad-501401, Telangana State, INDIA

*smanabol@gitam.edu

Abstract

Nano $[\text{Co}_3(\text{BTC})_2]$ (1) and $[\text{Zn}_3(\text{BTC})_2]$ (2) Metal-Organic Frameworks (MOFs) were synthesized using the mechano ball-milling method with cobalt or zinc metal salts and 1,3,5 benzene tricarboxylic acid (H_3BTC) as structural building unit. UV, IR, powder X-ray diffraction (PXRD), TGA and SEM analysis were employed to characterize 1 and 2. The average crystalline sizes evaluated by the Williamson-Hall equation from PXRD and SEM analysis suggest that 1 and 2 are in the range of 100-300 nm. The specific surface area of 1 and 2 was calculated by Brunauer–Emmett–Teller (BET) analysis and the pore size analysis by the BJH method.

We assessed the capability of the new nano MOFs as adsorbents for the desorption of methyl orange (MO) and methylene blue (MB). MOF 1 showed better efficiency and uptake capacity towards MO and MB within 30 min compared to MOF 2. We also evaluated the antimicrobial activity of the MOFs against *E. coli*, *Bacillus* and *Saccharomyces cerevisiae*. Both the MOFs exhibited good antimicrobial activity for up to 90 days, signifying the applicability of inhibition of bacteria in the preservation of food and drinking water.

Keywords: BTC-MOFs, Ball milling method, Water stable MOFs, BET analysis, Dye removal, Antimicrobial activity.

Introduction

With dwindling water resources and ever-increasing demand for drinking water, the chemical and biological pollution of water bodies through anthropogenic activities is posing a threat to sustainable growth and challenge to wastewater treatment approaches¹⁸. One such problem is the contamination of water by textile, leather, paper, printing, dyestuff and plastic industries discharged with a variety of chemicals, in particular dye materials^{2,3}. Several physical and chemical methods have been reported for removing the pollutants from contaminated water, while adsorption technology is one the viable, cost-effective approaches in treating large quantities of wastewater¹².

The contamination of water bodies by pathogens is another major environmental problem throughout the world for safe

drinking water. Antimicrobial agents are capable of destroying pathogenic microorganisms and are used to sterilize water and preserve food. Many drugs with antibacterial properties are in regular use¹⁹. Over the past decade, the microbial resistance to drugs has increased. Such drug resistance is a severe problem as microorganisms cause various diseases impacting on food storage, food packing, sterilization of medical instruments and implants. A drug-resistant infection in the brain could be life-threatening due to the inability of antibiotics to cross the blood-brain barrier²¹. Therefore, it becomes crucial to develop new potential antibacterial agents to fight resistant organisms continually.

The metal-organic frameworks (MOFs) have received substantial attention due to their high thermal stability, tunable pore size and other merits and enormous applications including in hydrogen storage³⁵, gas separation⁹, catalysis¹⁰ and sensing¹³. Biological applications of metal-organic frameworks (MOFs) in the fields of drug delivery²⁷, bio-sensing³⁸ and cosmetics are known^{6,7}. The ordered structures, biocompatibility and larger pore size of MOFs allow the storage of guest molecules and release metal ions slowly which make them desirable as adsorbents and antimicrobial materials⁸. MOFs namely MOF-5, HKUST-1, ZIF-8 and MOF-74 are known to possess excellent antimicrobial activity^{14,16}.

Cobalt and zinc metal ions at low concentrations exhibit low toxicity, but Zn shows increased toxicity at high presence. Cobalt with imidazole, Co (BDC) with 1,10 Phenanthroline, Co (BDC) with DABCO and zinc with hydrazinebenzoate ligands reportedly act as antimicrobial agents, with minimum inhibition for gram-positive and gram-negative bacteria in the range 2-20 mm at high concentrations^{2,11,23}.

We report the synthesis and characterization of $[\text{Co}_3(\text{BTC})_2]$ (1) and $[\text{Zn}_3(\text{BTC})_2]$ (2) nano MOFs by ball milling approach and investigated their ability for removal of methyl orange (MO) and methylene Blue (MB) as representative dyes. Further, their antimicrobial activity against *E. coli*, *Bacillus* and *Saccharomyces cerevisiae* was assessed to display potent activity.

Material and Methods

Methyl orange (MO), methylene blue (MB), Co $(\text{NO}_3)_2 \cdot 6\text{H}_2\text{O}$, Zn $(\text{NO}_3)_2 \cdot 6\text{H}_2\text{O}$ are supplied by S.D. Fine

Chemicals (India), DMF and BTC from Sigma Aldrich. All the above chemicals were used as received and without further purification.

Synthesis of 1 and 2 nano MOFs: Nano MOFs 1 and 2 were synthesized by mixing $\text{Co}(\text{NO}_3)_2 \cdot 6\text{H}_2\text{O}$ (0.296 mg, 1 mmol) or $\text{Zn}(\text{O}_2\text{CCH}_3)_2 (\text{H}_2\text{O})_2$ (0.219, 1 mmol) and 1,3,5 tri-carboxylic acid (BTC, 0.215 mg, 1 mmol) with 2 drops of DMF by using a high-energy planetary ball mill for 10 mins to form the homogenous powder at RT. The ratio (powder-to-ball) was 1:10 at 200 rpm and 10 mm tungsten carbide balls were used in milling. The products were washed with deionized water for 5 times and dried at 80°C for 3 hrs.

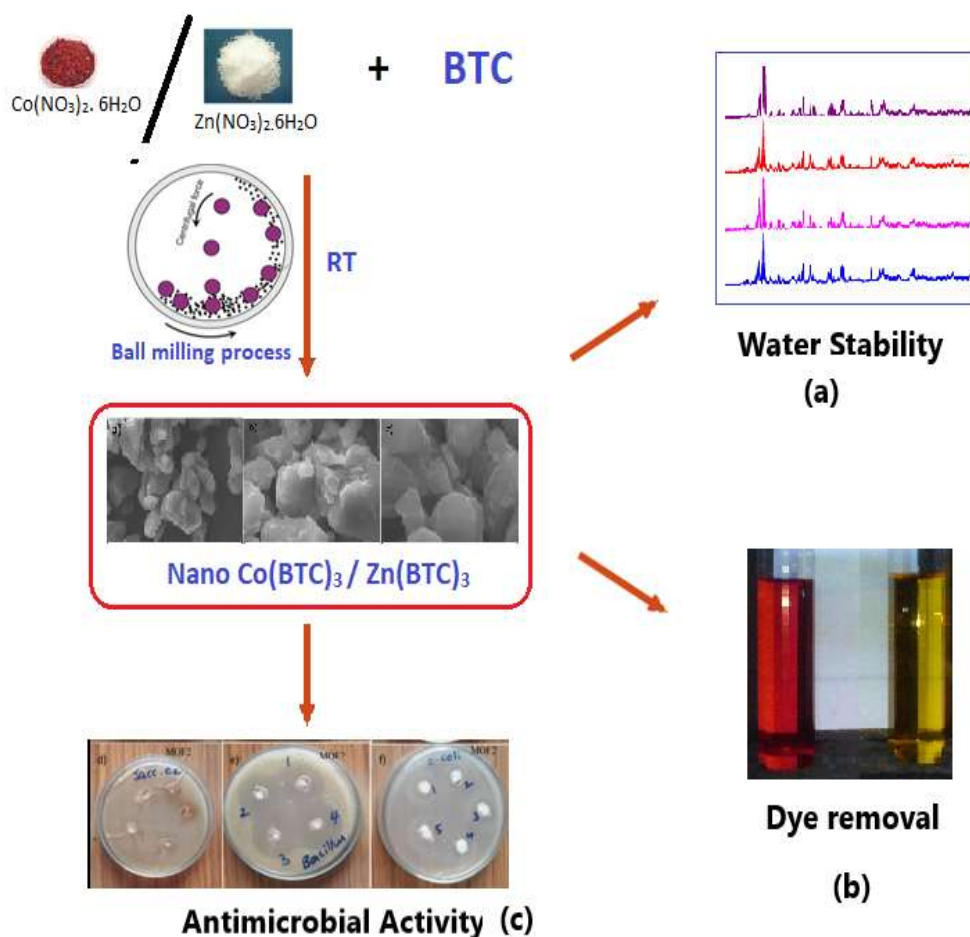
Antimicrobial activity: Agar diffusion method was described by Fiebelkorn et al⁶ used to evaluate the antibacterial and antifungal potential of MOF1 and 2 against *S. cerevisiae* (MTCC 170, baker's yeast), gram-negative bacteria, *E. coli* (MTCC 441) and gram-positive bacteria *Bacillus* (MTCC 443). Ciprofloxine was used as control and compared with liquid MOFs. Agar media was prepared²⁴ and mixed with antimicrobial cultures and poured into the Petri dishes for solidification. In the solidified agar media, holes were made with outside diameter 8.0 ± 0.1 mm, inside diameter 6.0 ± 0.1 mm (sterile borer).

Antimicrobial activity of MOF 1 and 2 was carried in liquid and solid-state; test samples were prepared with DMSO (1mg/ml) with concentrations of $2.5 \mu\text{g mL}^{-1}$, $5.0 \mu\text{g mL}^{-1}$, $10 \mu\text{g mL}^{-1}$ and $20 \mu\text{g mL}^{-1}$ solutions and $0.05 \mu\text{g}$, $0.10 \mu\text{g}$, $0.20 \mu\text{g}$ and $0.25 \mu\text{g}$ solid mass. Petri dishes were incubated at room temperature for 48 h at $35 \pm 2^\circ\text{C}$. After 48 h incubation, the diameter of zone inhibition was measured to evaluate the antimicrobial activity and plot the zone inhibition graphs.

Antioxidant activity of Cobalt and Zinc MOFs: The antioxidant activity of Cobalt and Zinc MOFs was estimated by using the DPPH assay process followed by the previous method^{15,30}. The radical scavenging ability of DPPH (0.001mM) with various volumes ($20, 40, 60, 80$ and $100 \mu\text{l}$) of MOF 1 and 2 with DMSO solution was added. To mix the above solutions, keep in the darkroom for 30 mins at RT, record the absorbance at 517 nm against a DPPH (blank) and ascorbic acid. Below equation determines the radical scavenging ability:

$$\text{DPPH Scavenging effect (\%)} = \frac{A_r - A_s}{A_r} \times 100$$

where A_r and A_s are absorbance ascorbic acid (reference) and test samples respectively.



Scheme 1: The schematic representation of synthesis nano MOFs (a) Water stability of 1 at 10 mins, 1hr, 15hr and 24 hrs (b) Removal of MO and MB (c) Antimicrobial activity of 1

Instrumentation: FT-IR spectra were recorded on spectrum GX spectrometer using KBr pellet (M/s, Perkin Elmer, USA) in a scan range of 4000-400 cm^{-1} . Scanning electron microscopy (SEM) sample images were taken on S-4800 (Hitachi) with a cold field emission gun. Powder X-ray diffraction (XRD) experiments were carried out on a Rigaku automatic diffractometer (ULTIMA-IV, 40 Kv, MA) with monochromatic Cu α radiation. Thermogravimetric analysis (TG) was conducted using a Neztch STA 449 F3 thermogravimetric analyzer. Samples were heated from 0 $^{\circ}\text{C}$ to 1000 $^{\circ}\text{C}$ at a rate of 10 $^{\circ}\text{C}/\text{min}^{-1}$ under a constant N_2 flow of 50 $\text{ml}/\text{min}^{-1}$. BET specific surface area and pore volumes were detected by N_2 physisorption at liquid nitrogen temperature (-196 $^{\circ}\text{C}$) using a Quantachrome NOVA 2000e sorption analyzer after the catalyst was degassed at 100 $^{\circ}\text{C}$ for 4hrs.

Results and Discussion

FT-IR spectra of MOF 1 and 2 are shown in fig. 1. The FT-IR spectra of 1 and 2 show two strong peaks between 1664 and 1390 cm^{-1} representing the stretching modes (symmetric and asymmetric vibrations) of the carboxylate group and the

benzene group as characteristic peaks of Co-BTC^{4,20} and Zn-BTC⁵. These peaks imply the coordination of the BTC format ligands with metal ions.

Further, the absences of intense peaks at 3050 cm^{-1} (-OH str), 1700 cm^{-1} (-C=O str) proves that-COOH groups of H_3BTC are deprotonated in 1 and 2 suggesting $-\text{COO}^-$ group in coordination with cobalt and zinc ions. Peaks observed at 569 cm^{-1} and 730 cm^{-1} are assigned to M-O stretching and 840-717 cm^{-1} for stretching vibrations of C-C groups and in-plane and out-of-plane deformation vibrations of the C-H groups in the benzene ring.^{26,28}

The crystalline powders of MOF 1 and 2 were characterized by using X-ray diffraction to verify the phase purity of the complexes. The 2θ range between 10.0-80.0 $^{\circ}$ illustrated in fig. 2. The XRD pattern of 1 shows peaks at 17.7, 18.8, 27.30, 28.70, 29.60, 33.40 $^{\circ}$ observed, which are consistent with previous reports.^{29,32,33} MOF 2 exhibits sharp, intense peaks (below 10 $^{\circ}$ 2θ values) around 10.9 (220), 13.4 (222), 16.4 (400), 18.5 (331), 19.3(420), 23.8(333) and 27.06 (202) observed and the values are matched with previous reports confirming purity and crystalline nature¹⁷ (Fig. 3S).

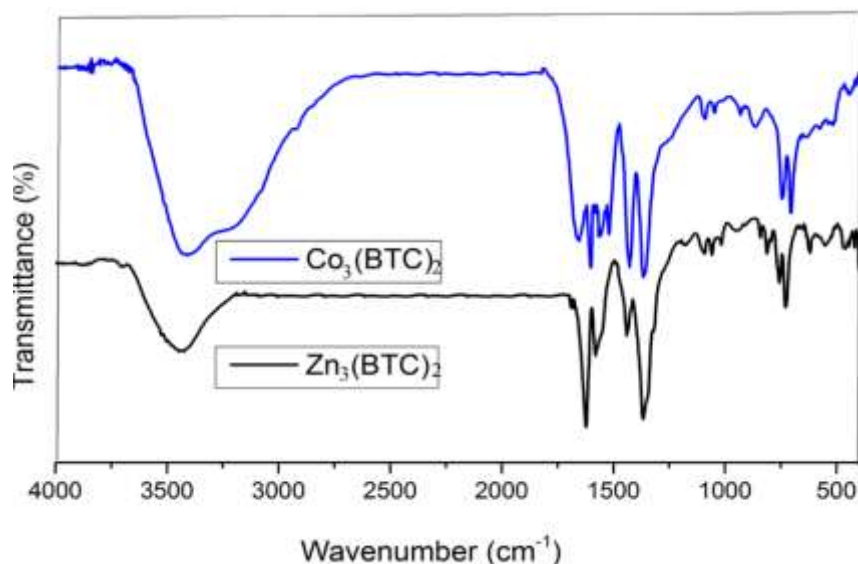


Fig. 1: FT-IR spectra of Cobalt MOF 1 and Zn MOF 2

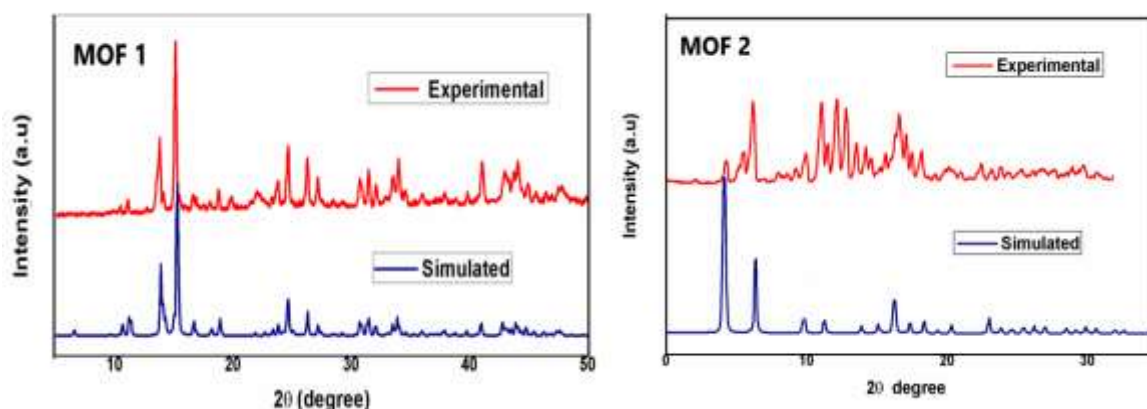


Fig. 2: PXRD graphs of simulated and synthesized MOF 1 and 2

Water stability studies: Aqueous stability of MOFs was evaluated through PXRD studies. 0.20 mg of a sample was taken in a test tube containing 10 ml of water and stirred for 10 min, 1h, 15 h and 20 h respectively (Scheme 1). PXRD patterns for each sample were measured after filtering, dried at 60-70°C for 6 h for removal of guest molecules. The average crystalline sizes evaluated by the Williamson-Hall equation for all the MOF 1 are 554(255) Å, 0.50(8) %; 552(396) Å, 0.4(1) %; 462(89) Å, 0.43(4) %; and -1339(427) Å, 0.14(4) % and MOF 2 size and strains are 3780(2436) Å, 0.34(8) %, with no major change up to 10 h in aqueous medium suggesting that these MOFs are stable in an aqueous medium (Figures 1S- 2S).

The size and morphology of 1 and 2 are characterized by SEM analysis (Fig. 3-4). In fig. 2, MOF 1 displayed homogenous spherical spongy pores and nanoplate shape

morphology with the distribution of particle size in the range 200-300 nm and average particle thickness of 75 ± 0.025 nm. While MOF 2 shows thin rods morphology with a rough surface area. The average particle size is from 150-300 nm approximately. Both powder XRD and SEM analysis suggest that both 1 and 2 are around 200-300 nm size.

TG and DTA analysis of 1 and 2 are carried after drying the samples at 70°C until no further weight loss is observed and results are shown in figure 5. Cobalt MOF 1 shows a sharp peak at 400-420°C due to decomposition the BTC ligand and the collapse of the MOF structure with the remaining CoO. Zinc MOF 2 shows weight loss at 420-460°C decomposition of the compound indicating the collapse of the whole framework. TG studies suggest that these nano MOFs are stable up to 400°C.

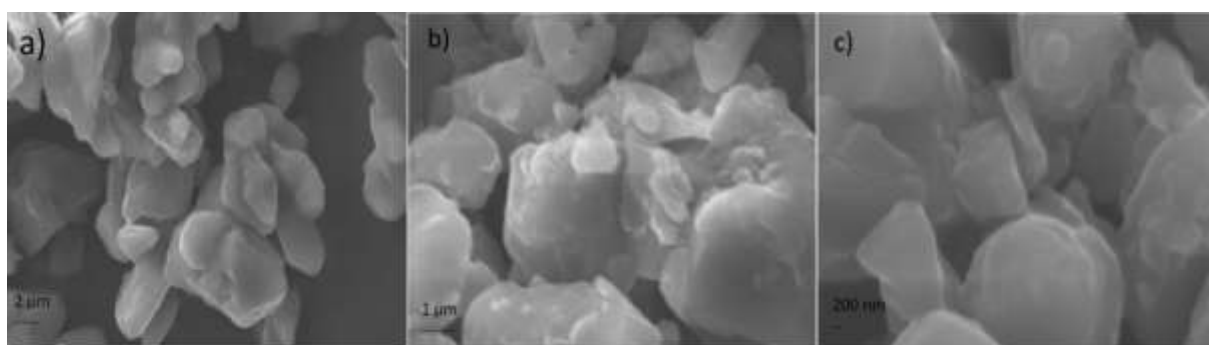


Fig. 3: SEM images of synthesized cobalt MOF 1

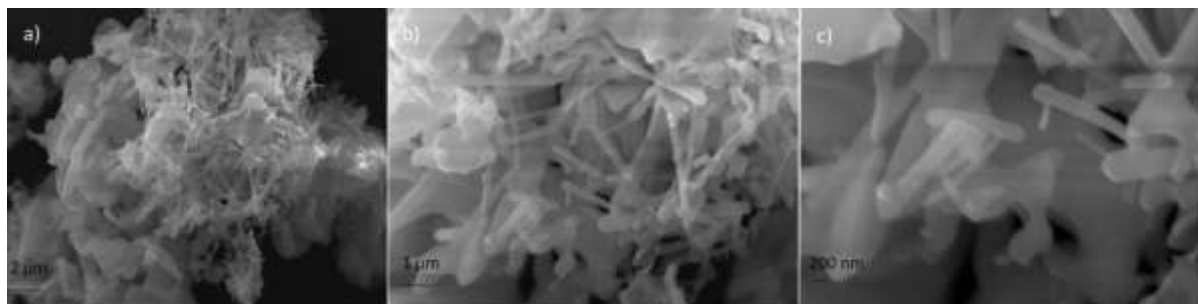


Fig. 4: SEM images of synthesized Zinc MOF

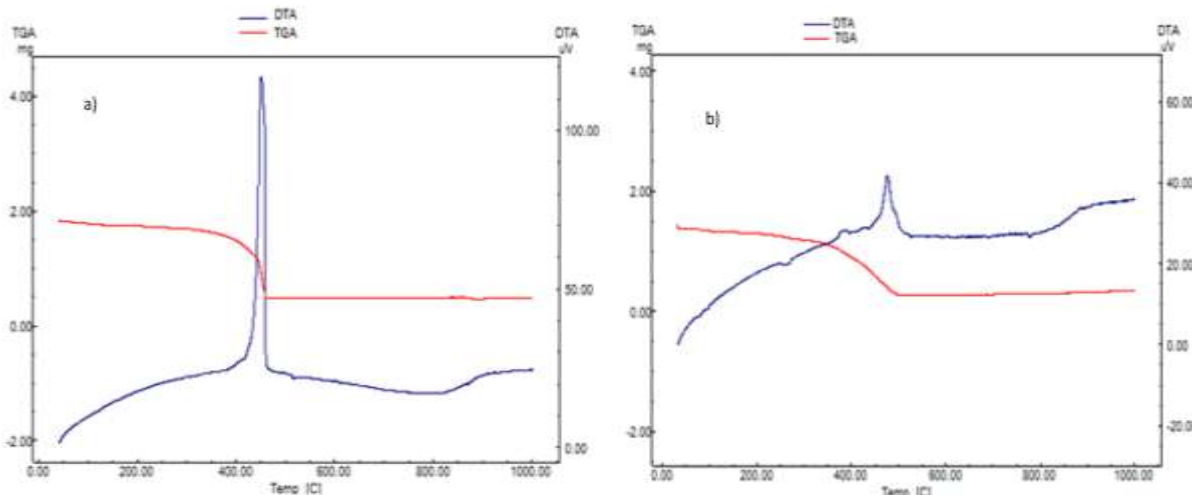


Fig. 5: (a) Thermogravimetric analysis of Cobalt MOF 1 (b) Zinc MOF 2

The BET analysis of 1 and 2 shows specific surface area and porosity properties by nitrogen adsorption measurements at 77°k. The N₂ adsorption-desorption isotherms of MOFs overlapped on the low pressure 0.03 (P/P_0) and high pressure is 0.9993 (P/P_0) indicating the high porosity of the materials. The linear BET curve data for 1 and 2 materials were with -4.970969E-08 (slope), 0.1298458 (intercept); -4.969019E-08(slope), 0.1299529 (intercept) respectively. The BET specific surface area and specific volumes of 1 and 2 are detected to be 62.87 m²/g, 0.057 cc/g; 38.34 m²/g, 0.045 cc/g respectively.^{31,34,37} The pore diameter distributions were calculated by the BJH method. The pore diameter region of two MOFs is 2-6 nm. The mean pore diameters are 2.7658 nm (1) and 1.5648 nm (2) respectively. Nitrogen adsorption, desorption graphs are shown in figure 6a, 7a and BJH graphs are shown in figures 6b, 7b.

Dyes Adsorption Studies: Dye adsorption and removal ability of 1 and 2 were estimated using MO and MB as representative dyes of polluted water by UV/Vis absorption studies. In figures 8a and 9a, the absorption intensity decreases from top to bottom with an increasing weight of 0.1 mg to 0.9 mg of 1, suggesting that removal of MO and MB increases with the increasing weight of 1. It is observed a maximum absorption at 0.9 mg of 1 on both MO and MB While 2 shows a very weak absorption even at 0.9 mg with MO and MB, this may be due to the replacement of cobalt with zinc which lacks ionic attraction³⁶.

Figures 8b and 9b illustrate the absorption spectra as a function of time MO and MB with 0.5 mg of 1. The decrease of absorption intensity with an increase in time, suggests that

removal of MO increases with an increase in contact time. Removal of MB with 0.50 mg of 1 after 24 h incubation showed a good result. The adsorption results with MOF 2 on both MO and MB are inferior. These results suggest that 1 acts as a better adsorbent for MO and MB removal, comparatively adsorption capacity is higher on MO and slow on MB dye, this may be the ionic attraction of 1.²⁵

Regeneration: Regeneration is carried with 10-15 ml of methanol by stirring for one hour at RT. After adsorption, the adsorbents were separated by centrifugation (10,000 rpm, 5 min), filtered and dried at 50°C for 5-6 h. The adsorption capacity of the regenerated samples was tested for 5 cycles (RT, PH-7) and compared to the first cycle. After five cycles, the removal efficiency of 1 was about 75%. Figure 10 shows that the adsorption capacity of MOF 1 for MO and MB decreases slowly in consecutive cycles. Among the two, MOF 1 is suitable for the effective removal of dyes (MO and MB) from wastewater.

From SEM images of 1 and 2, it is clear that 1 appears as spherical spongy morphology with the large surface area available for easy adsorption and desorption process while 2 shows thin rods morphology with a rough surface area not highly favourable for adsorption and desorption process. BET and TG analysis with a large porous area for easy adsorption supported and a sharp DTA peak suggesting no solvent molecules occupied the porous gaps. These all aspects favor the adsorption and desorption of MO and MB effectively by 1 than 2.

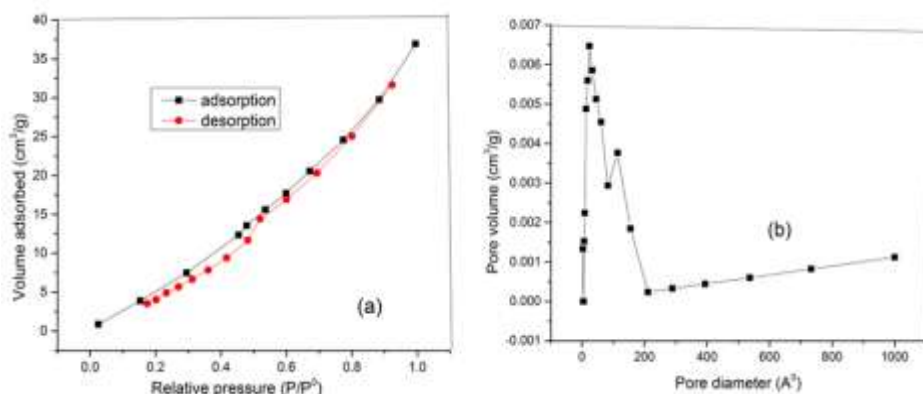


Fig. 6: (a) Adsorption, desorption graphs and (b) BJH graphs of Cobalt MOF1

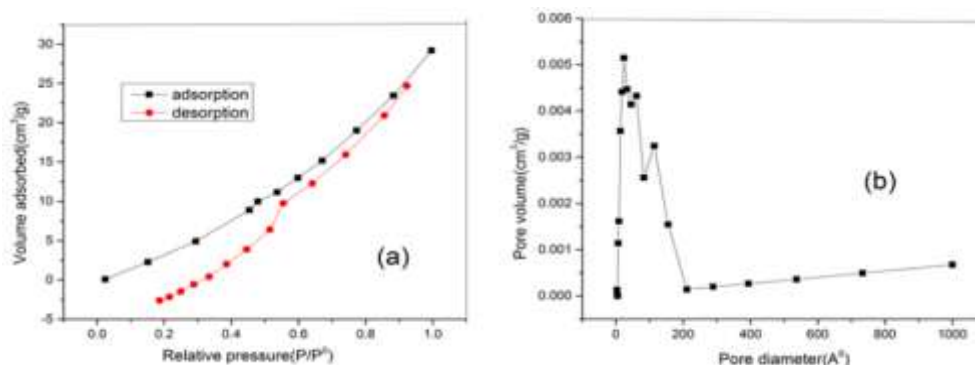


Fig. 7: (a) Adsorption, desorption graphs and (b) BJH graphs of Zinc MOF 2

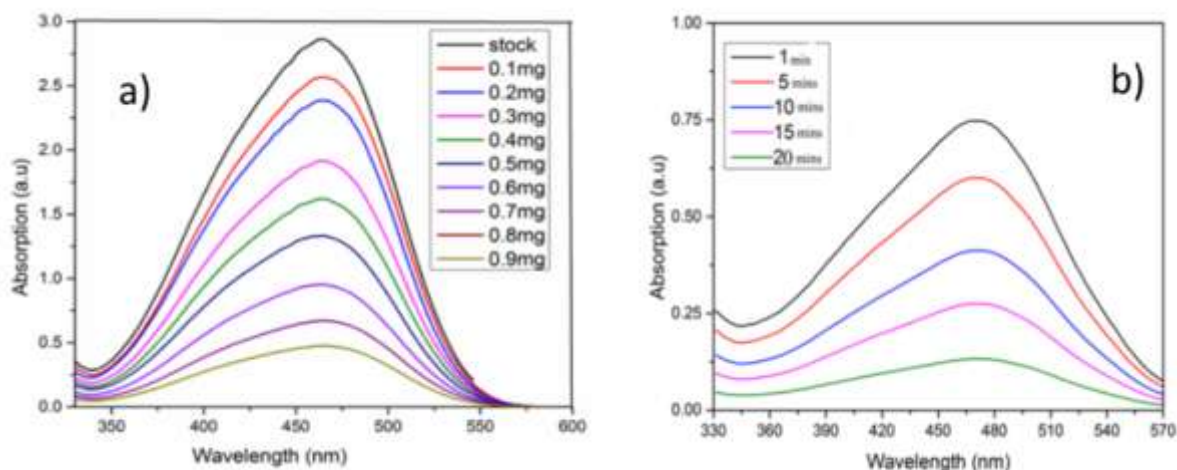


Fig. 8: UV-Vis spectra of the MO absorption ability of MOF 1 (a) Absorption spectra with 0.10 - 0.90 mg and (b) Spectra of MO as a function of time (1 to 20 min) with 0.50 mg of MOF 1

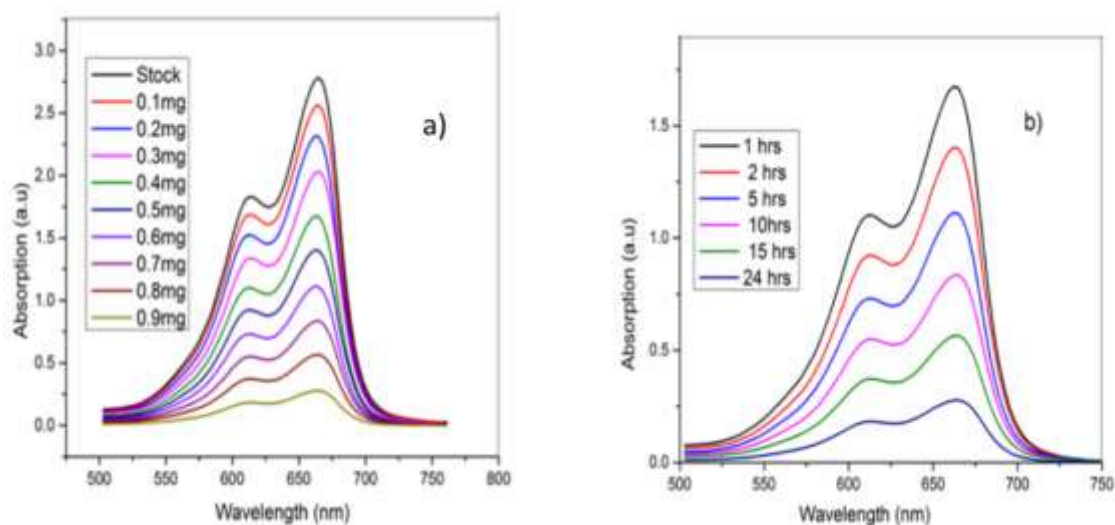


Fig. 9: UV-vis spectra of the dye absorption ability MOF 1 (a) Absorption spectra of MB with 0.10 - 0.90 mg (b) Spectra of MB as a function of time (1 to 24 hrs) with 0.50 mg of MOF 2

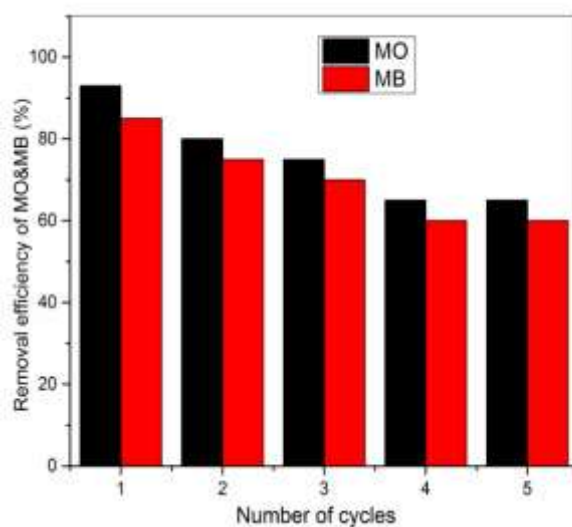


Fig. 10: MO and MB removal of the recycled MOF 1

Anti-microbial Activity: The antimicrobial activity was assessed by agar diffusion by the cup plate method with liquid MOFs (dissolved in DMSO) and agar diffusion method with solid MOFs. The cultures *Saccharomyces cerevisiae* (MTCC 170), *Bacillus subtilis* (MTCC 441) and *Escherichia coli* (MTCC 443) are used to evaluate the antimicrobial activity of MOF1 and 2 in sterile nutrient agar culture media.

In the agar diffusion method, MOF1 and 2 showed decent growth inhibition of microorganisms on *Saccharomyces cerevisiae* in liquid MOFs. While as prepared MOF1 and 2 compounds did not show activity against *bacillus* and *E. coli*. The results revealed that BTC ligands did not show antibacterial activity at low concentrations. The inhibition activity increased with an increase in the concentration of 1 and 2 as shown in figure 11.

The inhibition activity sustained even after seven days, possibly due to the presence of metal ions of MOF that dispersed in culture media uniformly over the wells. The diameter of the zone of inhibition in all dishes was recorded and corresponding inhibition curves are shown in figure 4S. The MOFs have exhibited superior inhibition activity even at lower concentrations compared with other BTC MOFs which may be due to better cation release tendency.³⁷

The prolonged antibacterial MOFs in solid form is carried to estimate ability in natural water and food preservation application purposes. MOFs 1 and 2 in solid form with different weights were placed directly onto the holes and inoculated agar plates at RT for initially for 24 h. After 24 hrs, the Petri plates were taken out to measure the zone of inhibition as shown in fig. 12. Excellent inhibition activity

was exhibited by both 1 and 2. Both MOFs showed excellent performance to inhibit the growth of the bacterial strains (inhibition diameter of around 15-30 mm) in solid form compared to the liquid state.

Further agar plates of the solid form of 1 and 2 were inoculated up to 90 days, showing almost similar consistent anti-microbial activity was displayed (Figure 5S and 6S). These results indicate that in solid form the anti-bacterial efficacy of the two MOFs is retained even after three months, which can be explained by their exceptional stability and possibly a slow release of metal ions in the presence of bacterial strains. Solid-state MOF 1 and 2 could inhibit the growth of microorganisms up to 90 days effectively suggesting that it can be explored for growth inhibition of bacteria in preservation of food and drinking water.

Anti-oxidation studies: The DPPH scavenging activity is one of the easy and fast methods for determination of antioxidant activity of synthesized MOF 1 and 2, using reference standard as ascorbic acid. Addition of MOF1&2 into the DPPH solution, the colour change was observed due to scavenging effect. Two MOFs had low scavenging at low concentrations. That the stable DPPH radical activity was increased with increase quantity of MOF 1 and 2 as shown in figure 14. These two MOFs scavenging rates show 20.2, 30.5, 40.7, 50.2, 60.5 and 20, 29.5, 36.5, 49.3, 58.9 at concentration as 20, 40, 60, 80, 100 μ l respectively. As a result, when compared with ascorbic acid, both MOFs have nearly equal scavenging activity and are used as antioxidant materials.

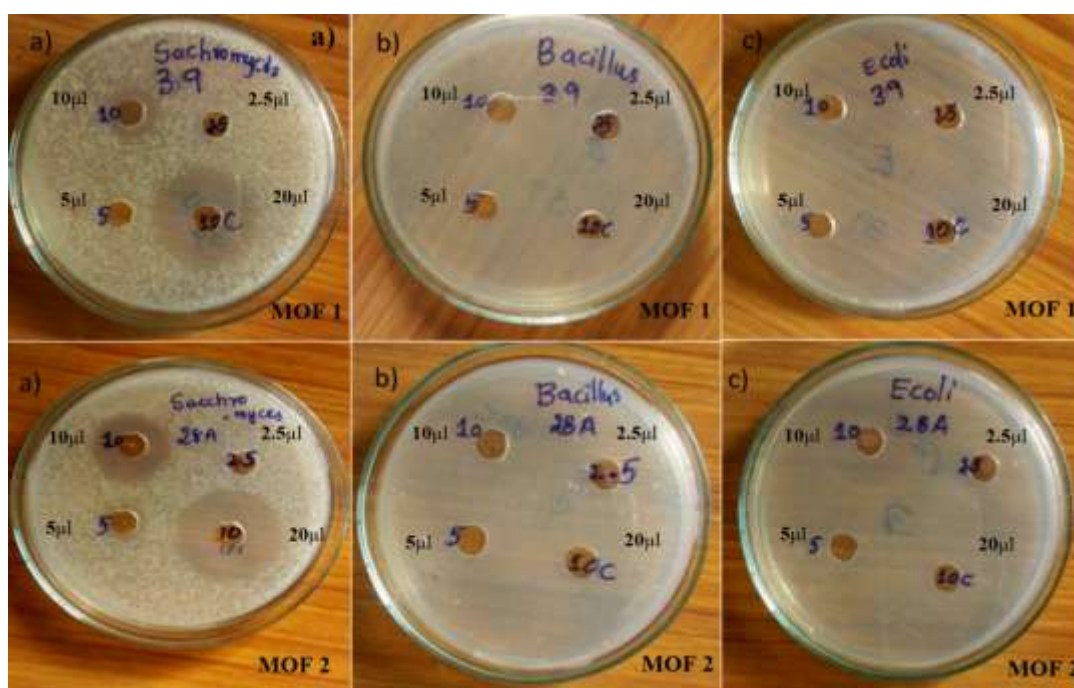


Fig. 11: Antimicrobial activity by Agar diffusion method on *Saccharomyces cerevisiae*, *Bacillus* and *E. Coli* by MOFs 1 and 2 with 2.5 μ g mL⁻¹, 5.0 μ g mL⁻¹, 10 μ g mL⁻¹ and 20 μ g mL⁻¹ at RT after 24 h incubation



Fig. 12: Antimicrobial activity by MOFs 1 and 2 with 0.05 µg, 0.10 µg, 0.15 µg, 0.20 µg and 0.25µg incubated at RT after 24hrs

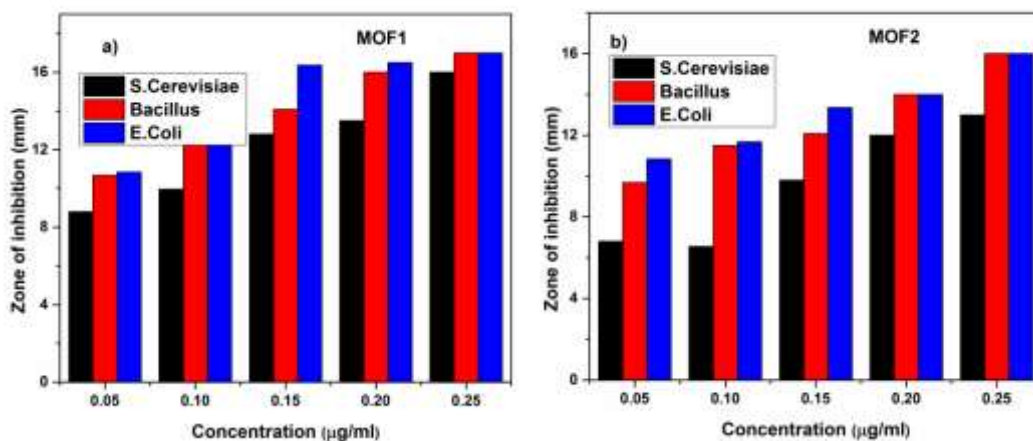


Fig. 13: The graphical representation of anti-microbial activity of MOF 1 and 2

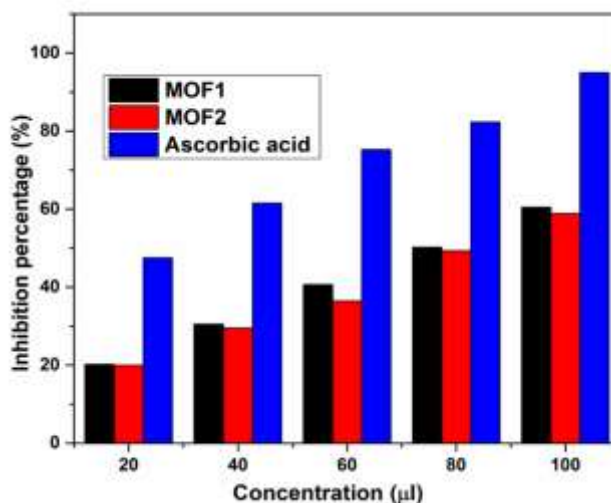


Fig. 14: Free radical scavenging activity of MOF 1 and 2

Supplementary

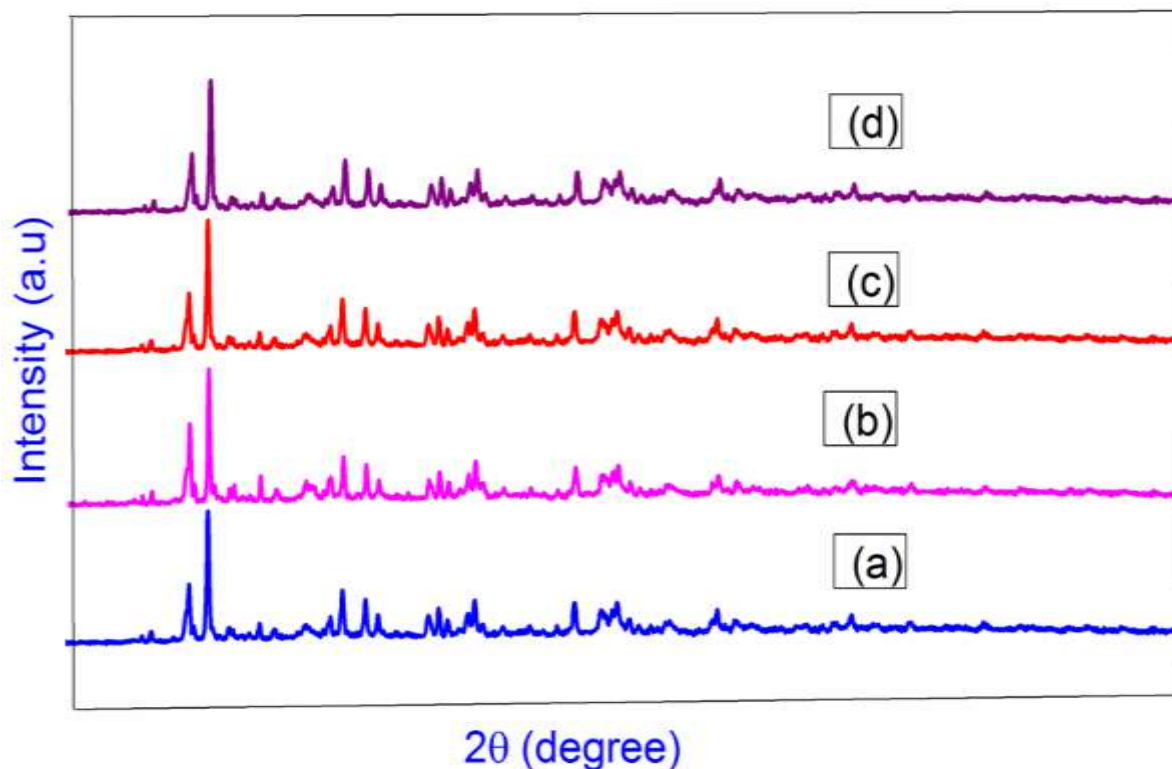


Fig. 1Sa: Water stability studies of MOF 1 at RT at different intervals of time using, XRD analysis (a) 10 min (b) 1hr (c) 15hrs and (d) 20hrs in water

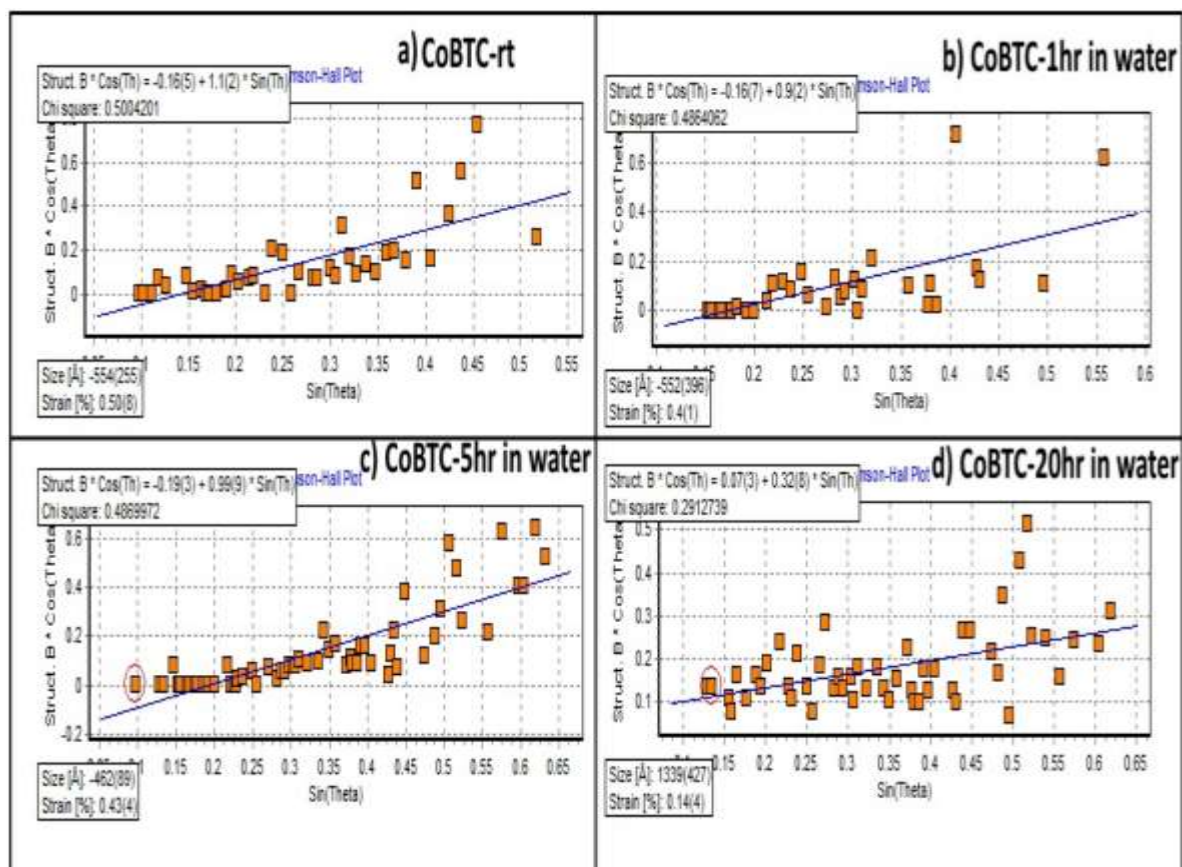


Fig. 1Sb: Williamson-Hall (W-H) profiles of the entire MOF 1

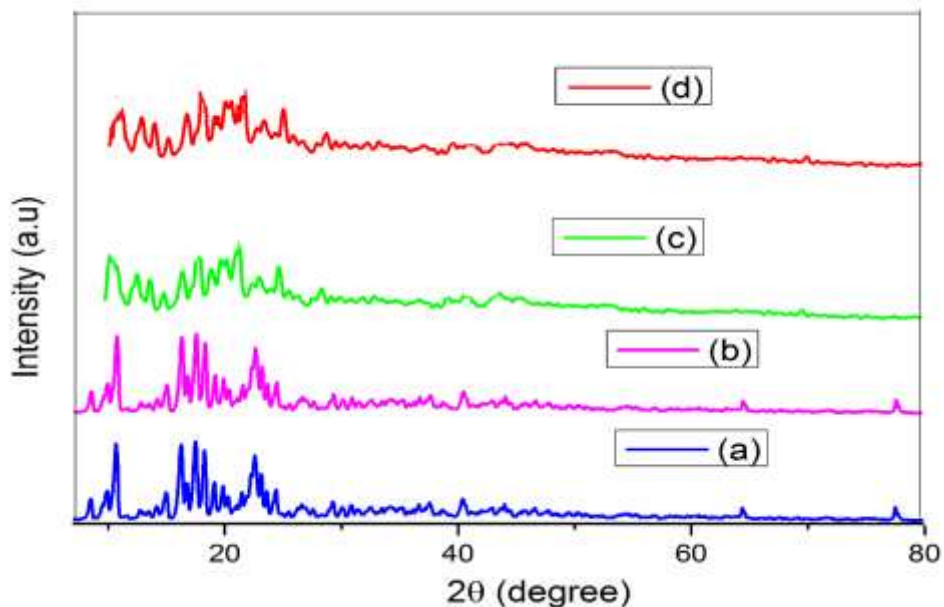


Fig. 2Sa: Water stability studies of MOF 2 at RT at different intervals of time using XRD analysis (a) 10 min (b) 1hr (c) 15hrs and (d) 20hrs in water

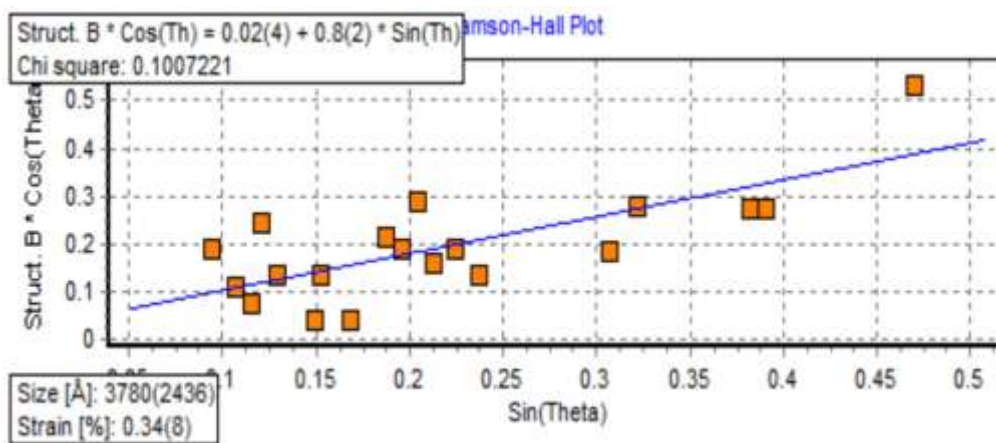


Fig. 2Sb: Williamson-Hall (W-H) profiles of the entire MOF 2

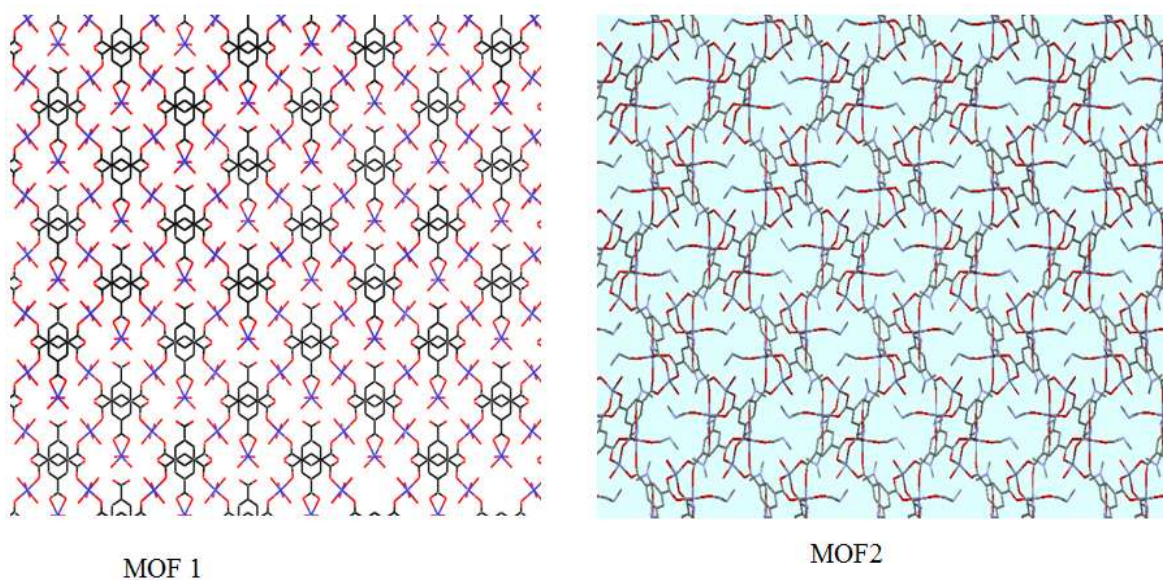


Fig. 3S: The structural arrangement MOF 1 and 2

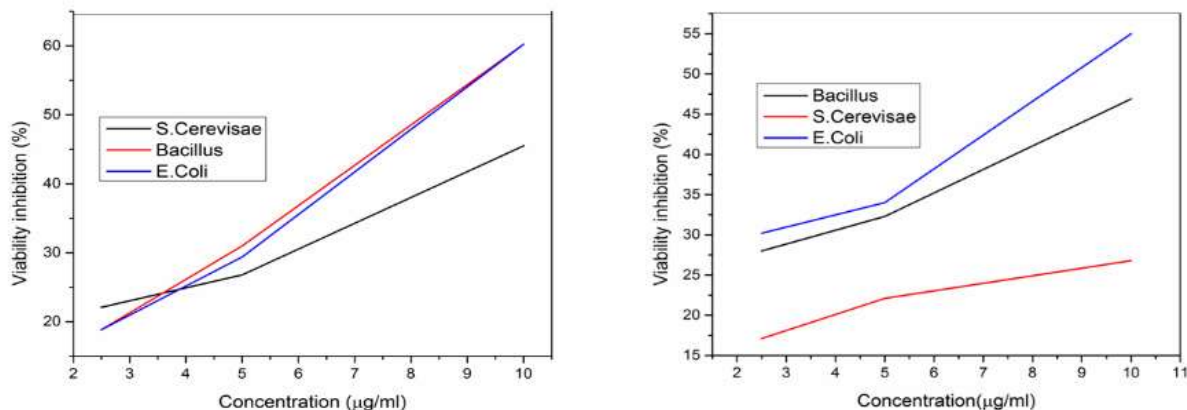


Fig. 4S: Viability inhibition of *Saccharomyces cerevisiae*, *Bacillus* and *E. Coli* with MOF 1 and 2, 48 hrs.

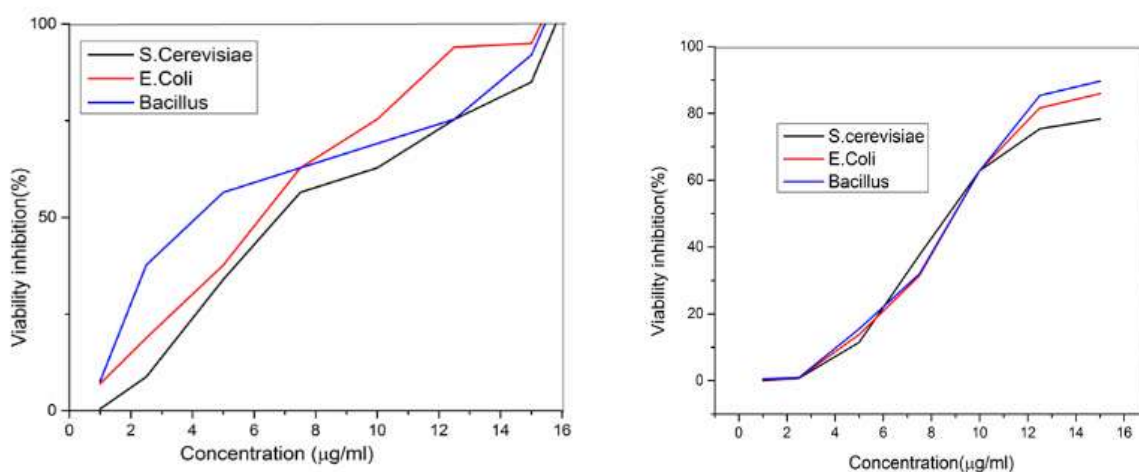


Fig. 5S: Viability inhibition of *Saccharomyces cerevisiae*, *Bacillus* and *E. Coli* with MOF 1 and 2, 48hrs

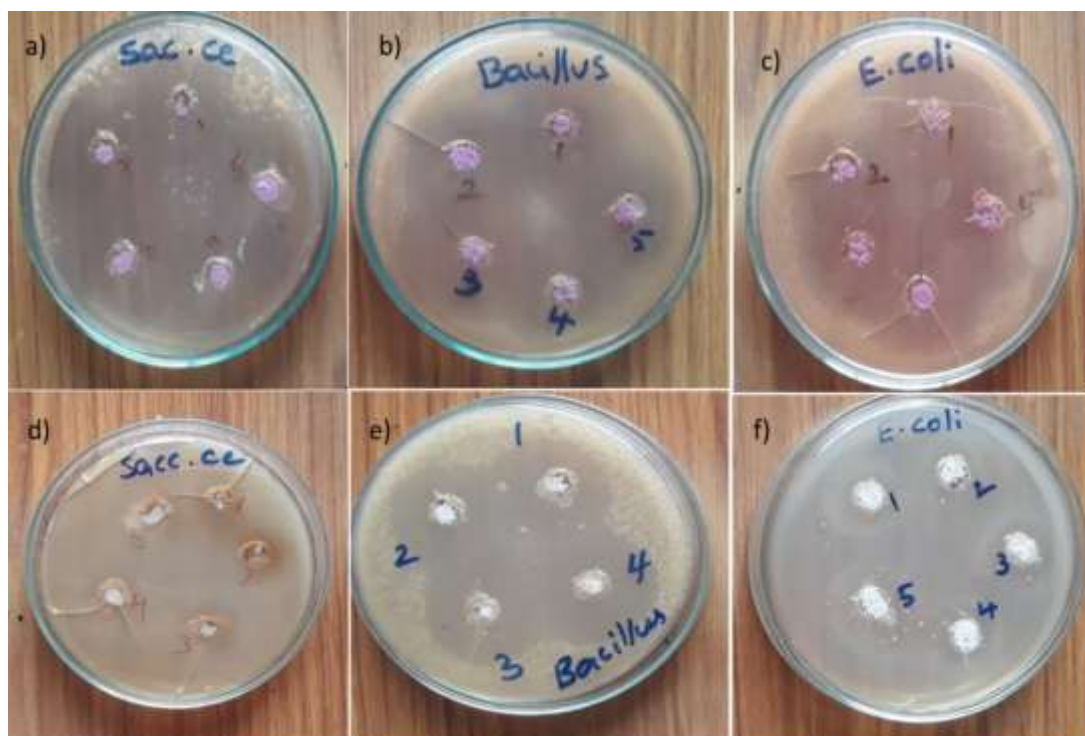


Fig. 6S: Estimation of antibacterial activity by Agar plate diffusion experiment carried on *Saccharomyces. cerevisiae*, *Bacillus* and *E. Coli cereus* with MOFs [$\text{Co}_3(\text{BTC})(1)$], [$\text{Zn}_3(\text{BTC})(2)$], [Incubation conditions, 303 K, 90 days]

Conclusion

Two Nano MOFs 1 and 2 are synthesized by the Mechano ball milling method with less energy and in short reaction times. Among the two, MOF 1 is suitable for the effective removal of dyes (MO and MB) from wastewater. MOF 1 can efficiently adsorb and remove the water-soluble molecules by the cationic absorption. Both MOFs showed excellent microbial inhibition activity obstructing the growth of *Saccharomyces cerevisiae*, *Bacillus* and *E. coli* both in solution phase and solid-state.

Solid-state MOF 1 could inhibit the growth of microorganisms up to 90 days effectively suggesting that it can be explored for growth inhibition of bacteria in preservation of food and drinking water.

Acknowledgement

The first author would like to thank Prof. Balaji Rao (GITAM University, Physics) for the lab facility of Mechano ball milling method and thanks To the Principal and Management of CMRP College for providing research facilities for anti-microbial activities.

References

1. Aguado S., Quirós J., Canivet J., Farrusseng D., Boltes K. and Rosal R., *Chemosphere*, **113**, 188 (2014)
2. Crini G., *Bioresour. Technol.*, **97(9)**, 1061 (2006)
3. Chen S., Zhang J., Zhang J., Yue K.Q., Li Y. and Li C., *Desalination*, **252(1-3)**, 149 (2010)
4. Cunha D., Yahia M.B., Hall S., Miller S.R., Chevreau H., Elkaïm E., Maurin G., Horcajada J. and Serre C., *Chem. Mater.*, **25(14)**, 2767 (2013)
5. Chinthamreddy A., Karreddula R., Pitchika G.K. and Surendra Babu M.S., *Journal of Inorganic and Organometallic Polymers and Materials*, **31(3)**, 1381-94 (2021)
6. Fiebelkorn K.R., Crawford S.A., McElmeel M.L. and Jorgensen J.H., *Journal of Clinical Microbiology*, **41(10)**, 4740 (2003)
7. Feldblyum J.I., Liu M., Gidley D.W. and Matzger A.J., *J. Am. Chem. Soc.*, **133(45)**, 18257 (2011)
8. Gangu K.K., Maddila S., Mukkamala S.B. and Jonnalagadda S.B., *Inorg. Chimica Acta*, **446**, 61 (2016)
9. Holman K.T., *Angew Chem. Int Ed.*, **50(6)**, 1228 (2011)
10. Horcajada P., Gref R., Baati T., Allan P.K., Maurin G., Couvreur P., Ferey G., Morris R.E. and Serre C., *Chem. Rev.*, **112(2)**, 1232 (2012)
11. He J., Zhang Y., Pan Q., Yu J., Ding H. and Xu R., *Micropor. Mesopor. Mat.*, **90(1-3)**, 145 (2006)
12. Haque E. et al, *J. Hazard Mater.*, **185(1)**, 507 (2011)
13. Jean S.S., Hsueh P.R., Lee P.S., Chang H.T., Chou M.Y., Chen I.S., Wang J.H., Lin L.F., Shyr J.M., Ko W.C., Wu J.J., Liu Y.C.,

Huang W.K., Teng L.J. and Liu C.Y., *Eur. J. Clin. Microbiol. Infect. Dis.*, **29(4)**, 471 (2010)

14. Janiak C. and Vieth J.K., *New J. Chem.*, **34(11)**, 2366 (2010)
15. Kitagawa S., Kitaura R. and Noro S., *Angew Chem. Int. Ed.*, **43(18)**, 2334 (2004)
16. Keskin S. and Kızılel S., *Ind. Eng. Chem.*, **50(4)**, 1799 (2011)
17. Kitagawa S. and Kitaura R., *Angew. Chem.*, **43(18)**, 2334 (2004)
18. Kora A.J. and Sashidhar R.B., *J. Antibiot.*, **68(2)**, 88 (2015)
19. Mittal A., Malviya A., Kaur D., Mittal J. and Kurup L., *Hazard J. Mater.*, **148(1-2)**, 229 (2007)
20. Mehta J., Bhardwaj N., Bhardwaj S.K., Kim K.H. and Deep A., *Coord. Chem. Rev.*, **322**, 30 (2016)
21. Mageshwari K. and Sathyamoorthy R., *Journal of Materials Science & Technology*, **29(10)**, 909-914 (2013)
22. Mohanta Y.K., Panda S.K., Jayabalan R. and Sharma N., *Front. Mol. Biosci.*, **4**, 1 (2017)
23. Peng L., Wu S., Yang X., Hu J., Fu X., Li M., Bai L., Huo Q. and Guan J., *New Journal of Chemistry*, **41(8)** 2891-2894 (2017)
24. Quiros J., Boltes K., Aguado S., De Villoria R.G., Vilatela J.J. and Rosal R., *Chem. Eng.*, **262**, 189 (2015)
25. Restrepo J., Serroukh Z., Santiago Morales J., Aguado S., Gomez Sal P., Mosquera M.E. and Rosal R., *Eur J. Inorg. Chem.*, **2017**, 574 (2017)
26. Sudik A.C., Cote A.P. and Yaghi O.M., *Inorg. Chem.*, **44(9)**, 2998 (2005)
27. Shen M., Forghani F., Kong X., Liu D., Ye X., Chen S. and Ding T., *Compr. Rev. Food Sci. Food Saf.*, **19(4)**, 1397-1419 (2020)
28. Sun K., Li L., Yu X., Liu L., Meng Q., Wang F. and Zhang R., *J. Colloid Interface Sci.*, **486**, 128 (2017)
29. Shi L., Hu L., Zheng J., Zhang M. and Xu J., *J. Disper. Sci. Technol.*, **37(8)**, 1226 (2016)
30. Singh M.P., Dhupal N.R., Kim H.J., Kiefer J. and Anderson J.A., *J. Phy. Chem. C.*, **120(31)**, 17323 (2016)
31. Sel K., Demirci S., Meydan E., Yildiz S., Ozturk O.F., Lohedan H.A. and Sahiner N., *J. Electron. Mater.*, **44(1)**, 136 (2015)
32. Schlichte K., Kratzke T. and Kaskel S., *Microporous and Mesoporous Materials*, **73(1-2)**, 81 (2004)
33. Tranchemontagne D.J., Hunt J.R. and Yaghi O.M., *Tetrahedron.*, **64(36)**, 8553 (2008)
34. Wu Y., Song X., Li S., Zhang J., Yang X., Shen P., Gao L., Wei R., Zhang J. and Xiao G., *Journal of Industrial and Engineering Chemistry*, **58**, 296-303 (2018)

35. Wei G., Feng L., Chang W., Zhang X., Jie-Ping L. and Qing-Yu G., *Cryst. Eng. Comm.*, **21(7)** 1159 (2019)

36. Xuan W., Ramachandran R., Zhao C. and Wang F., *Journal of Solid State Electrochemistry*, **22(12)**, 3873 (2018)

37. Xu W., Li G., Li W. and Zhang H., *RSC Advances*, **6(44)**, 37530 (2016)

38. Zeng G., Chen Y., Chen L., Xiong P. and Wei M., *Electrochimica Acta*, **222**, 773 (2016).

(Received 11th October 2020, accepted 04th January 2021)